IOP Publishing Journal of Physics: Condensed Matter
J. Phys.: Condens. Matter **32** (2020) 255603 (8pp) https://doi.org/10.1088/1361-648X/ab7c92

Entanglement and thermodynamic entropy in a clean many-body-localized system

Devendra Singh Bhakuni and Auditya Sharma[1]

Indian Institute of Science Education and Research, Bhopal, 462066, India

E-mail: devendra123@iiserb.ac.in and auditya@iiserb.ac.in

Received 13 January 2020, revised 17 February 2020
Accepted for publication 4 March 2020
Published 25 March 2020

Abstract

Whether or not the thermodynamic entropy is equal to the entanglement entropy of an eigenstate is of fundamental interest, and is closely related to the eigenstate thermalization hypothesis (ETH). However, this has never been exploited as a diagnostic tool in many-body-localized (MBL) systems. In this work, we perform this diagnostic test on a clean interacting system (subjected to a static electric field) that exhibits three distinct phases: integrable, non-integrable ergodic and non-integrable MBL. We find that in the non-integrable phase, the equivalence between the thermodynamic entropy and the entanglement entropy of individual eigenstates holds. In sharp contrast, in the integrable and non-integrable MBL phases, the entanglement entropy shows large eigenstate-to-eigenstate fluctuations, and differs from the thermodynamic entropy. Thus the non-integrable MBL phase violates ETH similar to an integrable system; however, a key difference is that the *magnitude* of the entanglement entropy in the MBL phase is significantly smaller than in the integrable phase, where the entanglement entropy is of the same order of magnitude as in the non-integrable phase, but with a lot of eigenstate-to-eigenstate fluctuations. Quench dynamics from an initial CDW state independently supports the validity of the ETH in the ergodic phase and its violation in the MBL phase.

Keywords: many-body-localized (MBL), entanglement entropy, eigenstate thermalization hypothesis (ETH), integrable systems

(Some figures may appear in colour only in the online journal)

1. Introduction

The question of how an isolated many-body system thermalizes has a long history. In the classical domain, thermalization of an isolated system in the limit of long times is governed by Boltzmann's ergodic hypothesis [1–3]. It states that classical chaotic systems, uniformly sample all the available micro-states at a given energy, in the long time limit. However, this hypothesis cannot be generalized directly to the quantum domain as in the long time limit the expectation value of an observable retains the initial memory of the system, and is thus unable to sample all the eigenstates of the system. Experimental advancement [4–6] in recent times has created a strong demand for a close understanding of thermalization in isolated quantum systems and led to a flurry of theoretical activity [7–16].

Thermodynamic entropy in the context of classical statistical mechanics is by its very nature an extensive quantity [1–3]. In quantum systems, entanglement entropy of individual eigenstates brings in a rich additional dimension. Discussions of the extensivity or the lack thereof of entanglement entropy have abounded [17–22] in recent times. The celebrated area law [23–25] which asserts that the ground state entanglement entropy scales with subsystem as the surface area of the subsystem, has been a central topic around which many of these studies have been carried out. However, the relationship between entanglement entropy and thermodynamic entropy has only been scantily covered [26]. In this letter, we demonstrate, with the aid of a specific example, that a systematic study of this relationship

[1] Author to whom any correspondence must be addressed.

is an illuminating diagnostic for a class of quantum phase transitions.

For an isolated quantum system it has been argued that the route to thermalization is described by the eigenstate thermalization hypothesis (ETH) [6, 27–30]. The ETH states that expectation values of operators in the eigenstates of the Hamiltonian are identical to their thermal values, in the thermodynamic limit. The measurement of any local observable in these systems gives the same expectation values for nearby energies. A closely related, but completely independent feature analogous to the ETH, is the question of whether the thermodynamic entropy of a subsystem obtained from the micro-canonical reduced density matrix with a fixed energy E_0 is equal to the entanglement entropy calculated from the energy eigenstate of the system with the same energy E_0 [26, 31].

The phenomenon of many-body-localization (MBL) [32–36] in which interactions fail to destroy Anderson localization (caused by random disorder) has created considerable excitement. The MBL phase is believed to exhibit properties similar to those of integrable systems [37–43]. In particular, although the ETH criterion is known to be satisfied by generic, non-integrable systems [8, 14, 44–50], a violation of the ETH is expected for integrable, and therefore MBL systems [7, 11, 26, 51]. The expectation value of any local observable in these systems fluctuates wildly for nearby eigenstates. Integrable systems are exactly solvable and have an extensive number of local conserved currents [52], which do not evolve in the course of time and hence prevent the system from thermalization. Similarly, MBL systems have conserved quasi-local integrals of motion which help to retain the memory of the initial state [40–43].

Most MBL systems have in-built disorder [35, 53, 54]. Recent work [55, 56] has proposed that a stable MBL-like phase may be obtained in a clean (disorderless) interacting system subjected to an electric field and a confining/disordered potential. The additional potential turns out to be essential as in its absence, the MBL phase cannot be obtained [55–58]. This many-body system is known to exhibit a rich phase diagram. In the absence of both electric field and curvature term, this model is integrable, while a finite value of either of these external potentials breaks the integrability. Further in the region of broken integrability it shows a transition from the ergodic to the MBL phase on varying the strength of the electric field. Thus it provides a good test bed to characterize various phases: integrable, non-integrable ergodic and non-integrable MBL phases. As opposed to a standard disordered system, a clean system could potentially be realized experimentally with greater ease, while still using the already available methods [59–63].

In this article, we demonstrate the profitability of a study of the relationship between thermodynamic entropy and entanglement entropy to characterize various phases. Although our technique is, in principle, more general, we concentrate on the concrete case of the above disorder-free model. We find that for a small subsystem, the entanglement entropy of each eigenstate matches with the thermodynamic entropy, provided the system is tuned in the non-integrable ergodic phase and satisfies the ETH criterion. However in the integrable and non-integrable MBL phases, the entanglement entropy shows large fluctuations for nearby eigenstates, and also differs from the thermodynamic entropy (figure 1 provides a schematic of these results). The difference between the thermodynamic entropy and the entanglement entropy increases on varying the strength of the electric field due to the strong localization from the electric field which leads to a smaller entanglement entropy. Further tests are done from an alternative perspective by studying the dynamics of average particle number in the subsystem. In the long time limit, the saturation value of the observable in the non-integrable ergodic phase matches with the results predicted by the diagonal ensemble and the micro-canonical ensemble, while in the non-integrable MBL phase the saturation value matches with the diagonal ensemble result but differs from the micro-canonical ensemble result.

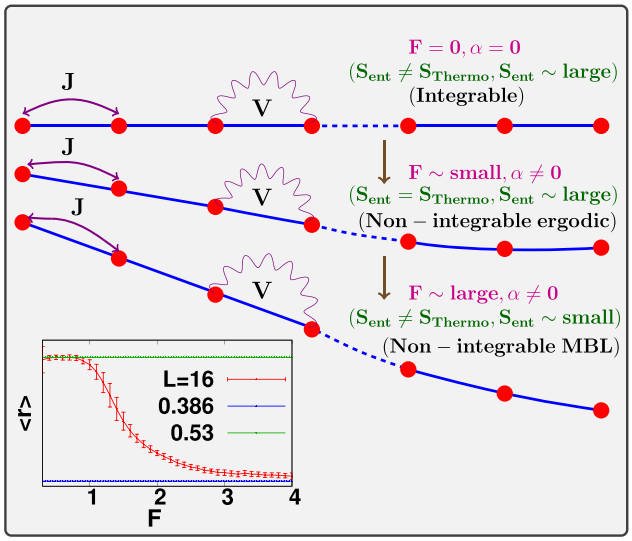

Figure 1. A schematic representation of the model with our main findings. In the non-integrable ergodic phase, the entanglement entropy matches with the thermodynamic entropy, while in the integrable and non-integrable MBL phases, it differs from the thermodynamic entropy. In the non-integrable MBL phase, the magnitude of the entanglement entropy is significantly smaller. The arrow represents the direction of increasing field strength. The inset shows the mean level-spacing ratio (averaged over different values of α) as a function of the field strength. The other parameters are: $L = 16$, $V = 1.0$ and filling factor $= 0.5$.

2. Model Hamiltonian

We consider a clean, spinless fermionic Hamiltonian with L sites [55]:

$$H = -J\sum_{j=0}^{L-2}(c_j^\dagger c_{j+1} + c_{j+1}^\dagger c_j) - F\sum_{j=0}^{L-1} j\left(n_j - \frac{1}{2}\right) + \alpha\sum_{j=0}^{L-1}\frac{j^2}{(L-1)^2}\left(n_j - \frac{1}{2}\right) + V\sum_{j=0}^{L-2}\left(n_j - \frac{1}{2}\right)\times\left(n_{j+1} - \frac{1}{2}\right), \quad (1)$$

where $c, c^\dagger$ are fermionic operators, F is the linear electric field, α is the curvature term and V is the nearest neighbor interaction. The curvature term (which has a factor of $\frac{1}{L^2}$) provides a slight non-linearity in the overall onsite potential, and helps break degeneracies [55]. The lattice constant is kept at unity and natural units ($J = \hbar = e = 1$) are adopted for all the calculations. In the non-interacting limit ($V = 0$) with $\alpha = 0$, the above Hamiltonian yields the Wannier–Stark ladder characterized by an equispaced energy spectrum proportional to the electric field strength, and where all the single particle eigenstates are localized [64, 65]. Furthermore, the dynamics governed by this Hamiltonian gives rise to oscillatory behavior which is known as Bloch oscillations [66–70]. When interactions are included, the model is integrable in the absence of both the static field and the curvature term ($F = 0, \alpha = 0$). The integrability is broken by a non-zero value of either the field F or the curvature α. When the field F is varied while keeping α fixed at a non-zero value, the system undergoes a transition from a delocalized (ergodic) phase at small field strengths to the MBL phase [55, 56] at large field strengths. The inset of figure 6 carries a plot of the mean level spacing ratio [71] (averaged over the curvature parameter α) as a function of the field, indicating a change of statistics [72] from Wigner–Dyson to Poisson.

3. ETH and thermodynamic entropy

For an isolated quantum system described by a Hamiltonian H, the time evolution of any initial state is given by

$$|\psi(t)\rangle = \mathrm{e}^{-\mathrm{i}Ht}|\psi(0)\rangle = \sum_n c_n \mathrm{e}^{-\mathrm{i}\epsilon_n t}|n\rangle, \tag{2}$$

where ϵ_n and $|n\rangle$ are the eigenvalues and the eigenstates of the Hamiltonian respectively. The information of the initial state is encoded into the coefficients c_n. For any operator $\hat{\mathcal{O}}$ the expectation value after any time t is given by

$$\langle\hat{\mathcal{O}}(t)\rangle = \langle\psi(t)|\hat{\mathcal{O}}(t)|\psi(t)\rangle. \tag{3}$$

Using equation (2), this simplifies to

$$\langle\hat{\mathcal{O}}(t)\rangle = \sum_n |c_n|^2\mathcal{O}_{nn} + \sum_{m\neq n} c_m^* c_n \mathrm{e}^{\mathrm{i}(\epsilon_m-\epsilon_n)t}\mathcal{O}_{mn}, \tag{4}$$

where $\mathcal{O}_{mn}$ are the matrix elements of the operator $\hat{\mathcal{O}}$ in the eigenbasis of the Hamiltonian H. It can be seen from equation (4) that in the long time limit ($t \to \infty$), generically (in the absence of degeneracy) the second term goes to zero and the expectation value of the observable saturates to the value predicted by the diagonal ensemble:

$$\langle\hat{\mathcal{O}}(t\to\infty)\rangle = \langle\hat{\mathcal{O}}_{\mathrm{DE}}\rangle = \sum_n |c_n|^2\mathcal{O}_{nn}. \tag{5}$$

Hence the system retains the memory of the initial state through the coefficients c_n, and does not follow the ergodic hypothesis.

Thermalization in isolated quantum many body systems happens via the mechanism of ETH, which implicitly involves the assumption that the diagonal elements of the operator $\hat{\mathcal{O}}$ change slowly with the eigenstates. Specifically, the off-diagonal elements $\mathcal{O}_{mn}$, and the difference in the neighboring diagonal elements: $\mathcal{O}_{n+1,n+1} - \mathcal{O}_{n,n}$ are exponentially small in $\mathcal{N}$, with $\mathcal{N}$ being the system size. With this assumption, the diagonal ensemble result (equation (5)) saturates to a constant value as the matrix elements $\mathcal{O}_{nn}$ are effectively constant over a given energy window.

Now considering the micro-canonical ensemble, the average value of the same observable can be written as

$$\langle\hat{\mathcal{O}}_{\mathrm{ME}}\rangle = \frac{1}{N_{\mathrm{states}}}\sum_{n=1}^{N_{\mathrm{states}}}\mathcal{O}_{nn}, \tag{6}$$

where N_{states} is the number of states in a given energy shell. Imposing the assumption of ETH, this also saturates to a constant value. Thus in the long time limit, the system thermalizes and the observable saturates to a thermal value predicted by the micro-canonical ensemble [6, 48, 49].

Under these conditions the expectation value of the operator $\hat{\mathcal{O}}$ in the energy eigenstate characterized by the density matrix $\rho_E \equiv |E\rangle\langle E|$ is the same as the micro-canonical average of the same operator:

$$\mathrm{Tr}(\rho_E\hat{\mathcal{O}}) = \mathrm{Tr}(\rho_{\mathrm{micro},E}\hat{\mathcal{O}}), \tag{7}$$

where the micro-canonical density matrix is defined as

$$\rho_{\mathrm{micro},E_0} = \frac{1}{N_{\mathrm{states}}}\sum_{E_0<E<E_0+\Delta E}|E\rangle\langle E|, \tag{8}$$

where N_{states} is the number of states available in the energy window ΔE. For a composite system $(A + B)$ characterized by the density matrix ρ, the entanglement entropy of a subsystem A is defined as: $S_{\mathrm{Ent}} = -\mathrm{Tr}(\rho_A \ln\rho_A)$, where $\rho_A = \mathrm{Tr}_B\rho$, is the reduced density matrix of the subsystem A taken after tracing out the degrees of freedom of the other subsystem B. On the other hand, the thermodynamic entropy from a micro-canonical ensemble is defined as: $S_{\mathrm{thermo}} = -\mathrm{Tr}(\rho_{\mathrm{micro}}\ln\rho_{\mathrm{micro}})$. The criterion of ETH is extended [26, 31] by asking whether the entanglement entropy of a small subsystem taken out of a large system in an eigenstate with energy E_0 is equal to the thermodynamic entropy computed from the micro-canonical density matrix (equation (8)) with the same energy E_0. Positing an ETH-like equation where ρ_{micro} is replaced by ρ_A we ask if the condition

$$S_{\mathrm{thermo}} = -\mathrm{Tr}(\rho_A\ \ln\ \rho_A) = -\mathrm{Tr}(\rho_{A,\mathrm{micro}}\ \ln\ \rho_{A,\mathrm{micro}}) \tag{9}$$

holds. Here, $\rho_{A,\mathrm{micro}}$ is the reduced density matrix corresponding to the micro-canonical density matrix ρ_{micro} ((equation (8)). For the subsystem A, this can be calculated by tracing out the degrees of freedom of the remaining part: $\rho_{A,\mathrm{micro}} = \mathrm{Tr}_B(\rho_{\mathrm{micro}})$.

Although the above criterion is analogous to the standard ETH one (equation (7)) the logarithmic factor $\ln\rho_A$ is not an observable quantity, thus making it an independent characteristic of thermalization. The appendix carries a short demonstration of the extensivity of thermodynamic entropy.

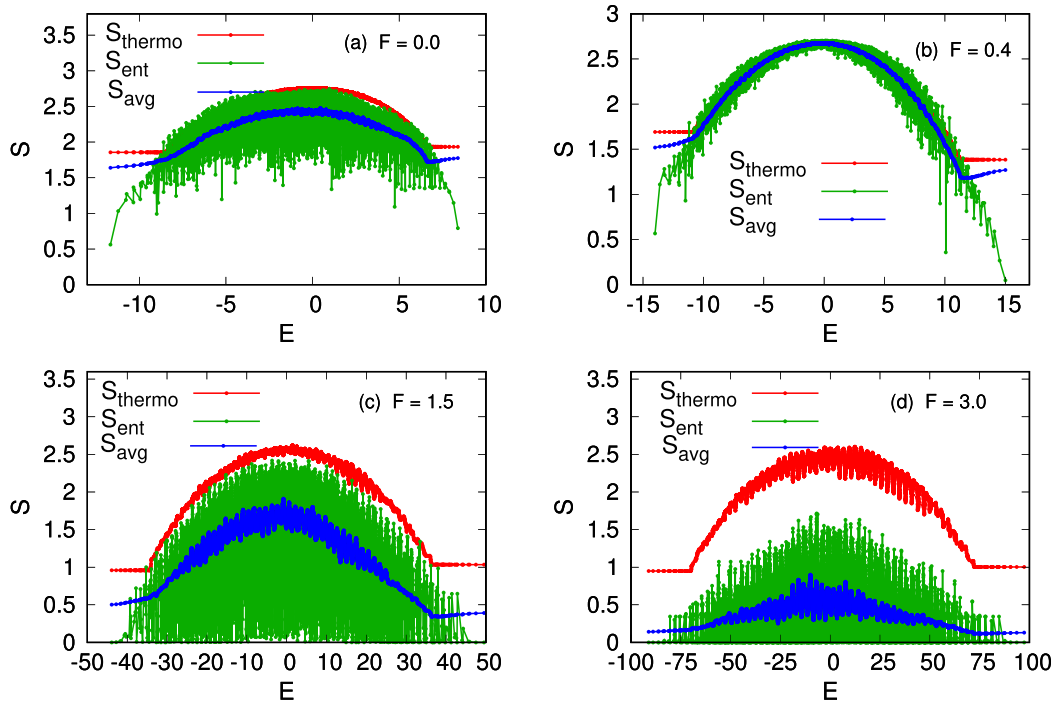

Figure 2. The entanglement entropy of each energy eigenstate and the corresponding thermodynamic entropy. (a) Integrable phase ($F = 0$, $\alpha = 0$): the entropy of nearby eigenstates fluctuates wildly with a finite difference between average entropy and the micro-canonical average. (b)–(d) Non-integrable phase: with $\alpha = 1.0$ and $F = 0.4$, 1.5, and 3.0 respectively. We obtain agreement between the entanglement entropy with its corresponding thermodynamic entropy in the ergodic phase ($F = 0.4$) satisfying ETH while the ETH is violated on increasing the value of field strength (going into the MBL phase). The other parameters are: $L = 16$, $V = 1.0$ filling factor $= 0.5$, and subsystem size $m = 4$.

4. Results and discussion

4.1. Statics

The model considered contains three regimes of interest: the integrable phase, the non-integrable ergodic phase and the non-integrable MBL phase. We employ numerical exact diagonalization of the model (equation (1)) for a system size upto $L = 16$ with the filling factor set to half filling. We also take the subsystem A to consist of the first m sites out of the L sites. We test the equivalence of the thermodynamic entropy and entanglement entropy (equation (9)) in these distinct phases. We compute the entanglement entropy for a small subsystem ($m = 4$) for all the eigenstates and plot it in figure 2. The thermodynamic entropy for all the eigenstates is also plotted by considering the micro-canonical density matrix (equation (8)), followed by tracing out the degrees of freedom of the complement of the subsystem. Since the energy spectrum fans out as a function of the electric field strength, we average the density matrix over $N_{\text{states}} = 100$ nearest-neighbor eigenstates to compute the thermodynamic entropy. Furthermore, the average entanglement entropy S_{avg} (average of the entanglement entropy of 100 nearby eigenstates) is also plotted in the same figure.

In the integrable case ($F, \alpha = 0$), the thermodynamic entropy differs from the entanglement entropy with the latter having a lot of fluctuations. However, for the parameters in the ergodic phase, nice agreement is found between the thermodynamic entropy and entanglement entropy, which signifies the validity of ETH in this phase. When the system is tuned on the border ($F = 1.5$), the entanglement entropy also shows fluctuations due to a mixture of both volume law and area law scaling states. This in-between phase has been called the 'S-phase' [73]. For the parameters in the MBL region, the entanglement entropy shows wild fluctuations and the thermodynamic entropy is also different from the entanglement

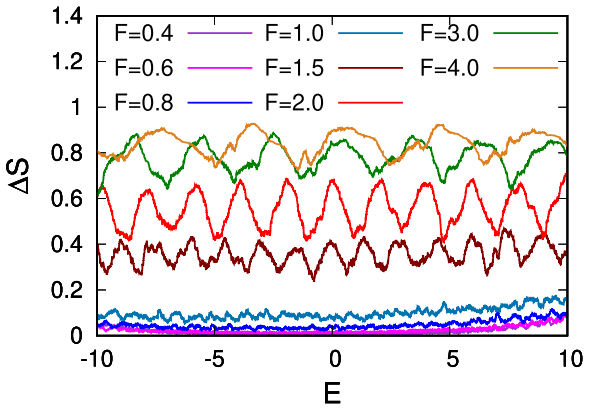

Figure 3. The difference between the thermodynamic entropy and the average entropy as a function of energy. Only the central part of the spectrum ($E \in [-10 : 10]$) is shown for various values of the field strength. In the ergodic phase the difference is almost zero while in the MBL phase the difference is much larger. The other parameters are: $L = 16$, $\alpha = 1.0$, $V = 1.0$ filling factor $= 0.5$, and subsystem size $m = 4$.

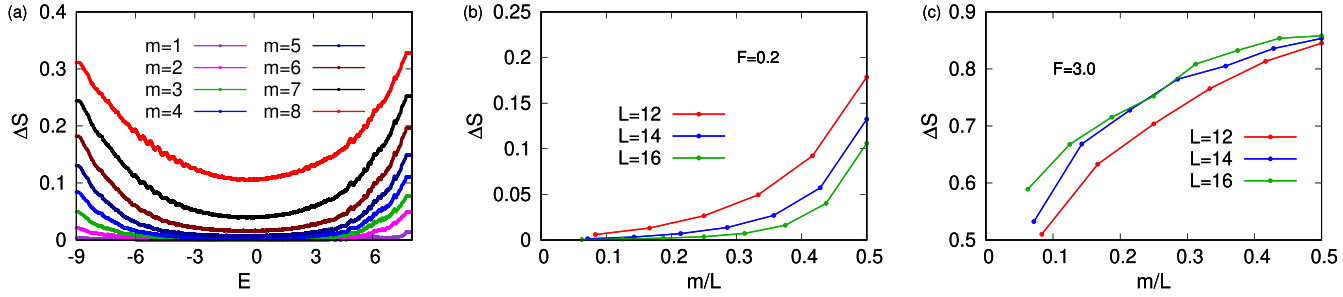

Figure 4. (a) Difference between the thermodynamic entropy and the average entropy (average carried out over 100 nearest eigenstates in both cases) as a function of energy for different subsystem sizes in the ergodic phase($F = 0.2$). A better thermalization can be seen for smaller subsystem sizes. (b) and (c) The finite size scaling of the difference of thermodynamic and average entropy (for a single eigenstate located at the middle of spectrum) as a function of the subsystem size in both ergodic and MBL phases. The other parameters are: $L = 16, \alpha = 1.0, V = 1.0$ filling factor $= 0.5$.

entropy, which suggests the breakdown of ETH in the MBL phase. It is interesting to note that even though both integrable and non-integrable MBL phases violate the ETH, the *magnitude* of entanglement is considerably lower in the latter, due to the underlying localization. It is useful to consider the difference between thermodynamic entropy and the average entanglement entropy:

$$\Delta S = \frac{S_{\text{thermo}} - S_{\text{avg}}}{S_{\text{thermo}}}. \tag{10}$$

The difference between the thermodynamic entropy and the entanglement entropy (ΔS) increases on increasing the electric field strength. The entropy for a part of the spectrum ($E \in [-10 : 10]$) is plotted in figure 3 for various values of the field strengths. In the ergodic phase the difference is close to zero signifying the validity of ETH while a finite difference in the MBL phase shows the violation of ETH.

Finally, we test the equivalence of thermodynamic entropy and entanglement entropy on varying the subsystem size. For each eigenstate, figure 4 shows the difference between these two for various values of subsystem size. It can be seen that for smaller subsystems the difference tends to zero, hence the smaller the subsystem the better is the thermalization [74, 75]. The other two figures in figure 4 show the finite size scaling of this difference but for a single eigenstate located at the center of the spectrum. It can be seen that for a smaller fraction m/L the difference goes to zero and thus shows the validity of ETH for these fractions. On the other hand, in the MBL phase, this difference is found to increase on increasing the system size as well as the subsystem sizes.

4.2. Quench dynamics

A complementary understanding of the distinction between the various phases is afforded by a study of the long time behavior of the system under time evolution. As evident from equation (4), the dynamics of any observable has two parts: the first part is the same as the result predicted by the diagonal ensemble while the second part gives the fluctuations around it. In the long time limit, the observable, in general, equilibrates to the diagonal ensemble value. However this does not imply the thermalization of the observable. An observable is said

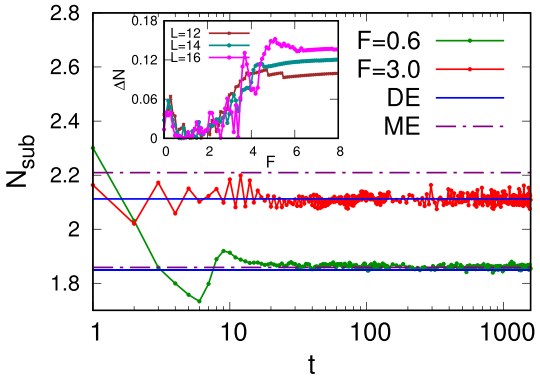

Figure 5. Quench dynamics: in the non-integrable ergodic phase ($F = 0.6$), the long time saturation value of the average number of particles in the subsystem matches with those of the diagonal ensemble and the micro-canonical ensemble. In the non-integrable MBL phase ($F = 3.0$) on the other hand, the saturation value matches with the result of the diagonal ensemble while it differs from that of the micro-canonical ensemble. The inset shows the normalized difference between the diagonal ensemble result and the micro-canonical ensemble result as a function of field strength for the same initial state. The value is close to zero in the non-integrable ergodic phase while a finite difference is obtained in the non-integrable MBL phase. The other parameters are: $L = 16, \alpha = 1.0, V = 1.0$ filling factor $= 0.5$, and subsystem size $m = 4$.

to thermalize if the result of the diagonal ensemble matches with the result predicted by any thermal ensemble such as micro-canonical or canonical.

We consider the average number of particles in the subsystem [76]: $\hat{\mathcal{O}} = \sum_{i=1}^{m} \hat{N}_i$, where $\hat{N}_i = c_i^\dagger c_i$ is the number operator at site i. The initial state is taken as a charge density wave state (where all the even sites are occupied and odd sites are empty), and the dynamics is governed by the final Hamiltonian (equation (1)). The prescription for obtaining the micro-canonical density matrix is as follows. We first calculate the average energy of the initial state: $E_{\text{ini}} = \langle\psi_0|H|\psi_0\rangle$. Next we obtain the eigenstate closest to this energy. By taking 100 nearest neighbor eigenstates around the obtained state, we then construct the micro-canonical density matrix.

We present data for the dynamics of the above observable in figure 5, comparing against the values predicted by the

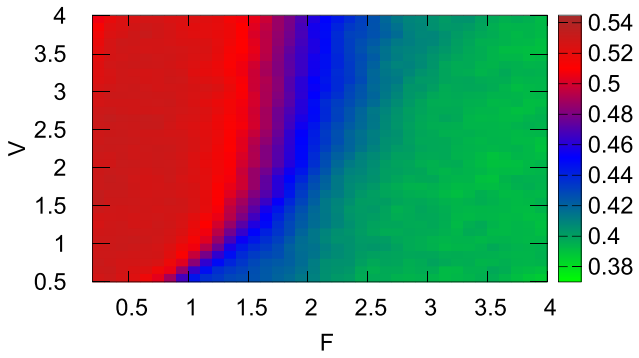

Figure 6. Surface plot of the level statistics as a function of both field strength (F) and the interaction strength (V). The other parameters are: $L = 16, \alpha = 1.0$.

diagonal and micro-canonical ensembles. In the ergodic phase, the long time limit of the expectation value of the observable is in agreement with that predicted by both the diagonal ensemble and the micro-canonical ensemble, which in turn implies thermalization and the validity of ETH in this phase. On the other hand, in the MBL phase the saturation value is the same as predicted by the diagonal ensemble but it differs from the micro-canonical ensemble result suggesting the lack of thermalization in the MBL phase. To study the difference between the diagonal and micro-canonical ensemble results, we define the following normalized difference:

$$\Delta N = \frac{|N_{\rm DE} - N_{\rm ME}|}{|N_{\rm ME}|}, \tag{11}$$

where $N_{\rm DE}$ and $N_{\rm ME}$ are the expectation values of the observable $\hat{\mathcal{O}}$, calculated from the diagonal ensemble and micro-canonical ensemble respectively. The inset shows the normalized difference ΔN (equation (11)) as a function of electric field strength for the same initial state. The value is close to zero in the non-integrable ergodic phase while a finite difference is obtained in the non-integrable MBL phase.

4.3. Variation of interaction strength

The nature of the phase obtained also depends on the interaction strength. Figure 6 shows the surface plot of the average level spacing as a function of both field strength and interaction strength for a fixed value of the curvature term ($\alpha = 1.0$). It can be seen that on increasing the interaction strength, the ergodic region extends, thus we expect the equivalence of the entanglement entropy and the thermodynamic entropy to hold in this extended region.

5. Summary and conclusions

To summarize, we test the validity of ETH in an interacting system subjected to a static electric field. For small electric field strength this model shows ergodic behavior while for sufficiently strong electric field it exhibits MBL. In the limit of zero electric field and curvature strength, the model is integrable. We find that in the ergodic phase, the entanglement entropy of the states following a volume law of scaling matches with the corresponding thermodynamic entropy thus satisfying the ETH criterion, while in the MBL phase, the entanglement entropy fluctuates wildly from eigenstate to eigenstate, and also differs from the thermodynamic entropy. Since the MBL phase possesses low entanglement, a clear distinction is obtained between the integrable and the MBL phase from the point of view of the ETH. As reported earlier [26], a striking distinction between integrable and non-integrable systems is the presence of large eigenstate-to-eigenstate fluctuations in the expectation value of any observable in the integrable case. In support of the argument that the MBL phase is similar to integrable systems, we find that indeed, the MBL phase is also characterized by large flucutations in entanglement entropy across adjacent eigenstates. However, in contrast to the integrable phase, the *magnitude* of entanglement is significantly lower in the MBL phase. Moreover, the difference between the average entropy and the thermodynamic entropy increases on going deep into the localized phase.

We further verify the above arguments from a dynamical perspective by studying the dynamics of average number of particles in the subsystem starting from a charge density wave type of initial state. We find that in the ergodic phase the saturation value obtained from the dynamics, the result predicted by the diagonal ensemble as well as the micro-canonical ensemble result match with each other, implying that the system thermalizes in the long time limit. In the MBL phase on the other hand, the saturation value matches with the result predicted by the diagonal ensemble, but differs from that predicted by the micro-canonical ensemble. This signifies the lack of thermalization or ETH in the MBL phase.

Acknowledgments

We are grateful to the High Performance Computing (HPC) facility at IISER Bhopal, where large-scale calculations in this project were run. A S is grateful to SERB for the grant (file number: CRG/2019/003447), and for financial support via the DST-INSPIRE Faculty Award [DST/INSPIRE/04/2014/002461]. D S B acknowledges PhD fellowship support from UGC India. We are grateful to Josh Deutsch and Sebastian Wüster for their comments on the manuscript. We thank Ritu Nehra for help with the schematic diagram.

Appendix A. Scaling of entanglement entropy and thermodynamic entropy

In this appendix, we show the scaling of entanglement entropy and thermodynamic entropy of two random states from the middle of the spectrum as a function of subsystem size. In the ergodic phase ($F = 0.2$), both the entropies match with each other and follow a volume law scaling, while in the MBL phase ($F = 3.0$), only the thermodynamic entropy shows a volume law scaling (figure A1).

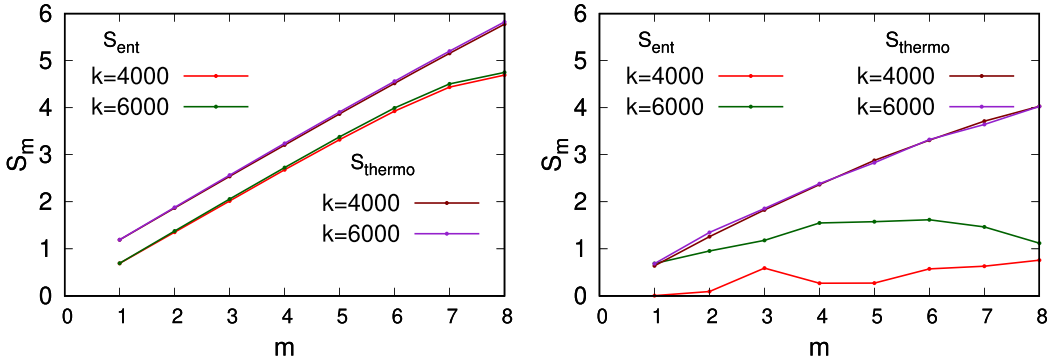

Figure A1. The scaling of entanglement entropy and thermodynamic entropy as a function of subsystem size for two different eigenvectors in the middle of the spectrum (randomly choosen to be states with eigen-indices $k = 4000$, and $k = 6000$ respectively). In the ergodic phase ($F = 0.2$), both follow volume law scaling (left). The thermodynamic entropy is shifted by an amount 0.5 to make it distinguishable. In the MBL phase ($F = 3.0$), only the thermodynamic entropy shows a volume law scaling (right). The other parameters are: $L = 16, \alpha = 1.0$ and $V = 1.0$.

ORCID iDs

Devendra Singh Bhakuni https://orcid.org/0000-0003-3603-183X

References

[1] Huang K 2009 *Introduction to Statistical Physics* (London: Chapman and Hall)
[2] Pathria R and Beale P 2011 *Statistical Mechanics* (Amsterdam: Elsevier)
[3] Penrose O 1979 *Rep. Prog. Phys.* **42** 1937
[4] Kinoshita T, Wenger T and Weiss D S 2006 *Nature* **440** 900
[5] Hofferberth S, Lesanovsky I, Fischer B, Schumm T and Schmiedmayer J 2007 *Nature* **449** 324
[6] Rigol M, Dunjko V and Olshanii M 2008 *Nature* **452** 854
[7] Rigol M 2009 *Phys. Rev. Lett.* **103** 100403
[8] Santos L F and Rigol M 2010 *Phys. Rev.* E **82** 031130
[9] Rigol M and Fitzpatrick M 2011 *Phys. Rev.* A **84** 033640
[10] He K and Rigol M 2012 *Phys. Rev.* A **85** 063609
[11] Mondaini R and Rigol M 2015 *Phys. Rev.* A **92** 041601
[12] Beugeling W, Moessner R and Haque M 2014 *Phys. Rev.* E **89** 042112
[13] Rigol M, Dunjko V, Yurovsky V and Olshanii M 2007 *Phys. Rev. Lett.* **98** 050405
[14] Santos L F and Rigol M 2010 *Phys. Rev.* E **81** 036206
[15] Canovi E, Rossini D, Fazio R, Santoro G E and Silva A 2011 *Phys. Rev.* B **83** 094431
[16] Rigol M and Santos L F 2010 *Phys. Rev.* A **82** 011604
[17] Vitagliano G, Riera A and Latorre J I 2010 *New J. Phys.* **12** 113049
[18] Wolf M M 2006 *Phys. Rev. Lett.* **96** 010404
[19] Lai H-H, Yang K and Bonesteel N E 2013 *Phys. Rev. Lett.* **111** 210402
[20] Roy N and Sharma A 2018 *Phys. Rev.* B **97** 125116
[21] Roy N, Sharma A and Mukherjee R 2019 *Phys. Rev.* A **99** 052342
[22] Pouranvari M and Yang K 2014 *Phys. Rev.* B **89** 115104
[23] Hastings M B 2007 *J. Stat. Mech.* P08024
[24] Laflorencie N 2016 *Phys. Rep.* **646** 1
[25] Eisert J, Cramer M and Plenio M B 2010 *Rev. Mod. Phys.* **82** 277
[26] Deutsch J, Li H and Sharma A 2013 *Phys. Rev.* E **87** 042135
[27] Deutsch J M 1991 *Phys. Rev.* A **43** 2046
[28] Srednicki M 1994 *Phys. Rev.* E **50** 888
[29] Deutsch J M 2018 *Rep. Prog. Phys.* **81** 082001
[30] D'Alessio L, Kafri Y, Polkovnikov A and Rigol M 2016 *Adv. Phys.* **65** 239
[31] Deutsch J 2010 *New J. Phys.* **12** 075021
[32] Gornyi I V, Mirlin A D and Polyakov D G 2005 *Phys. Rev. Lett.* **95** 206603
[33] Basko D M, Aleiner I L and Altshuler B L 2006 *Ann. Phys.* **321** 1126
[34] Anderson P W 1958 *Phys. Rev.* **109** 1492
[35] Nandkishore R and Huse D A 2015 *Annu. Rev. Condens. Matter Phys.* **6** 15
[36] Pal A and Huse D A 2010 *Phys. Rev.* B **82** 174411
[37] Vosk R and Altman E 2013 *Phys. Rev. Lett.* **110** 067204
[38] Huse D A, Nandkishore R and Oganesyan V 2014 *Phys. Rev.* B **90** 174202
[39] Vasseur R and Moore J E 2016 *J. Stat. Mech.* 064010
[40] Abanin D A, Altman E, Bloch I and Serbyn M 2019 *Rev. Mod. Phys.* **91** 021001
[41] Imbrie J Z, Ros V and Scardicchio A 2017 *Ann. Phys.* **529** 1600278
[42] Serbyn M, Papić Z and Abanin D A 2013 *Phys. Rev. Lett.* **111** 127201
[43] Chandran A, Kim I H, Vidal G and Abanin D A 2015 *Phys. Rev.* B **91** 085425
[44] Khatami E, Rigol M, Relano A and García-García A M 2012 *Phys. Rev.* E **85** 050102
[45] He K, Santos L F, Wright T M and Rigol M 2013 *Phys. Rev.* A **87** 063637
[46] Tang B, Iyer D and Rigol M 2015 *Phys. Rev.* B **91** 161109
[47] Beugeling W, Moessner R and Haque M 2014 *Phys. Rev.* E **89** 042112
[48] Kim H, Ikeda T N and Huse D A 2014 *Phys. Rev.* E **90** 052105
[49] Rigol M and Srednicki M 2012 *Phys. Rev. Lett.* **108** 110601
[50] Ikeda T N, Watanabe Y and Ueda M 2013 *Phys. Rev.* E **87** 012125
[51] Khatami E, Rigol M, Relaño A and García-García A M 2012 *Phys. Rev.* E **85** 050102
[52] Sutherland B 2004 *Beautiful Models: 70 Years of Exactly Solved Quantum Many-Body Problems* (Singapore: World Scientific)
[53] Luitz D J, Laflorencie N and Alet F 2015 *Phys. Rev.* B **91** 081103
[54] Iyer S, Oganesyan V, Refael G and Huse D A 2013 *Phys. Rev.* B **87** 134202
[55] Schulz M, Hooley C, Moessner R and Pollmann F 2019 *Phys. Rev. Lett.* **122** 040606
[56] van Nieuwenburg E, Baum Y and Refael G 2019 *Proc. Natl Acad. Sci.* **116** 9269
[57] Moudgalya S, Prem A, Nandkishore R, Regnault N and Bernevig B A 2019 arXiv:1910.14048

[58] Taylor S R, Schulz M, Pollmann F and Moessner R 2019 arXiv:1910.01154
[59] Schreiber M, Hodgman S S, Bordia P, Lüschen H P, Fischer M H, Vosk R, Altman E, Schneider U and Bloch I 2015 *Science* **349** 842
[60] Choi J-y, Hild S, Zeiher J, Schauß P, Rubio-Abadal A, Yefsah T, Khemani V, Huse D A, Bloch I and Gross C 2016 *Science* **352** 1547
[61] Smith J, Lee A, Richerme P, Neyenhuis B, Hess P W, Hauke P, Heyl M, Huse D A and Monroe C 2016 *Nat. Phys.* **12** 907
[62] Kondov S, McGehee W, Xu W and DeMarco B 2015 *Phys. Rev. Lett.* **114** 083002
[63] Bordia P, Lüschen H, Scherg S, Gopalakrishnan S, Knap M, Schneider U and Bloch I 2017 *Phys. Rev.* X **7** 041047
[64] Krieger J and Iafrate G 1986 *Phys. Rev.* B **33** 5494
[65] Wannier G H 1960 *Phys. Rev.* **117** 432
[66] Bouchard A and Luban M 1995 *Phys. Rev.* B **52** 5105
[67] Mendez E E and Bastard G 1993 *Phys. Today* **46** 34
[68] Hartmann T, Keck F, Korsch H and Mossmann S 2004 *New J. Phys.* **6** 2
[69] Bhakuni D S and Sharma A 2018 *Phys. Rev.* B **98** 045408
[70] Bhakuni D S, Dattagupta S and Sharma A 2019 *Phys. Rev.* B **99** 155149
[71] Oganesyan V and Huse D A 2007 *Phys. Rev.* B **75** 155111
[72] Atas Y, Bogomolny E, Giraud O and Roux G 2013 *Phys. Rev. Lett.* **110** 084101
[73] Xu S, Li X, Hsu Y-T, Swingle B and Sarma S D 2019 arXiv:1902.07199
[74] Vidmar L, Hackl L, Bianchi E and Rigol M 2017 *Phys. Rev. Lett.* **119** 020601
[75] Vidmar L, Hackl L, Bianchi E and Rigol M 2018 *Phys. Rev. Lett.* **121** 220602
[76] Li X, Ganeshan S, Pixley J H and Das Sarma S 2015 *Phys. Rev. Lett.* **115** 186601